World Academy of Science, Engineering and Technology
International Journal of Mechanical and Mechatronics Engineering
Vol:6, No:1, 2012

Elasto-Visco-Plastic-Damage Model for Pre-Strained 304L Stainless Steel subjected to Low Temperature

Jeong-Hyeon Kim, Ki-Yeob Kang, Myung-Hyun Kim, and Jae-Myung Lee

***Abstract*—**Primary barrier of membrane type LNG containment system consist of corrugated 304L stainless steel. This 304L stainless steel is austenitic stainless steel which shows different material behaviors owing to phase transformation during the plastic work. Even though corrugated primary barriers are subjected to significant amounts of pre-strain due to press working, quantitative mechanical behavior on the effect of pre-straining at cryogenic temperatures are not available. In this study, pre-strain level and pre-strain temperature dependent tensile tests are carried to investigate mechanical behaviors. Also, constitutive equations with material parameters are suggested for a verification study.

***Keywords*—**Constitutive equation, corrugated sheet, pre-strain effect, elasto-visco-plastic-damage model, 304L stainless steel

I. Introduction

LIQUEFUED natural gas (LNG) has received great attention as an alternative fuel of oil and fossil coal to reduce greenhouse gas emissions. Under these circumstances, the size of LNG containment systems is increased, and concerns for safety design have been increased. Independent spherical tank systems and membrane tank systems have become the mainstream of LNG containment systems due to their reliability and economic efficiency. In membrane type containment systems, corrugated 304L stainless thin steel with 1.2mm thickness is using as a primary barrier to absorb sloshing impact and fatigue loads. When fabricating corrugated stainless sheet, a flat type plate is folded through press working, and plastic deformation phenomenon take place [1]–[3]. As a result, mechanical properties for origin material can be changed but there were few consideration of pre-strain effect when membrane type LNG cargo containment design procedures.

In this study, uni-axial tensile test was carried out to investigate the effect of pre-strain of 304L stainless steel at ambient temperatures and cryogenic temperatures.

Jeong-Hyeon Kim is with the Department of Naval Architecture & Ocean Engineering, Pusan National University, Busan, South Korea, (phone: +82-51-510-3986; e-mail: honeybee@pusan.ac.kr).

Ki-Yeob Kang is with the Department of Naval Architecture & Ocean Engineering, Pusan National University, Busan, South Korea, (phone: +82-51-510-3986; e-mail: kgyup15@pusan.ac.kr).

Myung-Hyun Kim is with the Department of Naval Architecture & Ocean Engineering, Pusan National University, Busan, South Korea, (phone: +82-51-510-2486; e-mail: kimm@pusan.ac.kr).

Jae-Myung Lee is with the Department of Naval Architecture & Ocean Engineering, Pusan National University, Busan, South Korea, (phone: +82-51-510-2342; fax: +82-51-512-8836; e-mail: jaemlee@pusan.ac.kr).

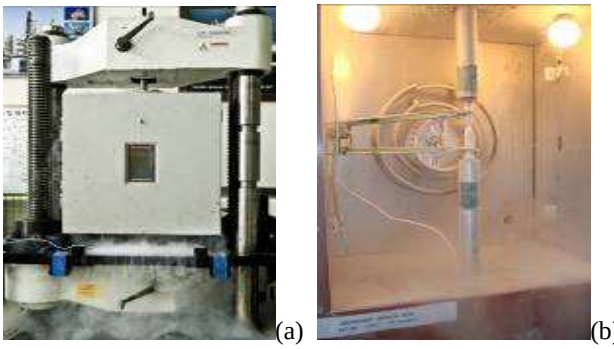

(a) (b)

Fig. 1 (a) Universal testing machine and (b) cryogenic tensile test

Fig. 2 Test specimen shape and dimension (KS B0801 10)

In addition, pre-strain dependent unified elasto-visco-plastic constitutive model and new method for determining material constants are proposed.

II. Experiments

A. Experimental Equipment

Chemical composition of tested 304L stainless steel is shown in Table I. In order to investigate the effect of pre-straining on 304L stainless steels, a custom-built mechanical testing system was used in this experiment. A universal testing machine (UH 1000KNI, SHIMADZU) equipped with a cryogenic chamber (up to -200°C) was used (Fig. 1). Nitrogen gas was operated to create cryogenic environment in the chamber with three thermocouples. To ensure the test results, cryogenic extensometer (3542-050M-100-LT, Epsilon Tech) was embedded into the specimen in the cryogenic chamber. Fig. 2 shows the test specimen shapes and dimensions of 304L stainless steel.

TABLE I
Chemical Composition of 304L Stainless Steel

	Chemical composition (%)								
304L	C	Cr	Si	Cu	P	Mn	Ni	S	Mo
	0.016	18.2	0.376	0.5	0.028	1.451	8.63	0.0251	0.254

TABLE II
EXPERIMENTAL CONDITIONS FOR TENSILE TEST

Type	No.	Temperature		Pre-strain
		Pre-strain	Re-loading	
As-Received	1	293K		0 %
	2	110K		0 %
AL test	3	293K	110K	5 %
	4			10 %
	5			13 %
	6			16 %
	7			19 %
	8			22 %
LL test	9	110K	110K	5 %
	10			10 %
	11			13 %
	12			16 %
	13			19 %
	14			22 %

B. Experimental Conditions

The percentage of pre-strained amount is varied from 5% to 22% at ambient temperatures and cryogenic temperatures. AL test represents that pre-strained at ambient temperatures and low temperature re-loading. LL test means pre-strained at low temperatures and low temperature re-loading. All the specimens tested at low temperatures carried out pre-cooling for 30 minutes. In addition, all the pre-strained specimens prepared at a low temperature were stored for two weeks at ambient temperature to allow for full elastic recovery. Table II shows the tensile test conditions. Each experiment has been performed three times for a reliable result.

III. EXPERIMENTAL RESULTS

The stress-strain curves for the AL and LL tests are shown in Fig 3(a) and (b), respectively. The AL test results show the well known TRIP behavior, which is the most important mechanical behavior of austenitic stainless steel at low temperatures [4].

The AL test results shown in Fig 3(a) indicate that there is no increase in the tensile strength when compared to the yield strength. This indicates that the tensile strength of austenitic stainless steel is not dependent on the amount of pre-strain when the pre-strain is induced at ambient temperature. In other words, the maximum load-carrying capacity of austenitic stainless steel-based structures, which can sustain significant amounts of pre-strain induced by metal press processing, is not affected by the pre-strain when they are used in a low-temperature environment. However, this does not hold true in the case of cyclic loading at low temperatures, because the pre-strain is

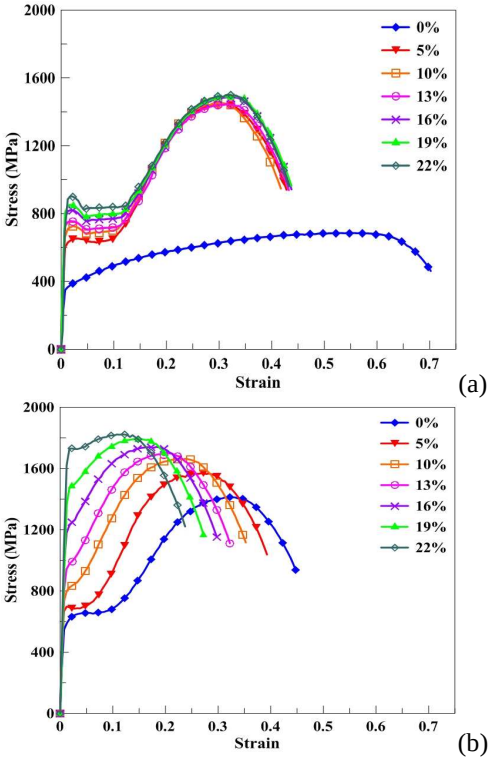

Fig. 3 Pre-strain dependent stress-strain relationship of 304L stainless steel (a) AL test results (b) LL test results

induced at ambient temperature. In this context, the effect of pre-strain induced at a low temperature should be analyzed.

Fig 3(b) shows the stress-strain relationship of the LL test results. In contrast to the AL test results shown in Fig 3(a), the LL test results indicate an increase in the yield as well as tensile strength. An increase in the amount of pre-strain resulted in an increase in both the yield as well as tensile strength.

IV. CONSTITUTIVE MODEL

It is well known that the amount of phase transformation quantities affect the plastic deformation characteristics significantly, so a number of researches are conducted to measure phase transformation. Because TRIP phenomena can be analyzed numerically by incorporating the phase transformation equation into the constitutive model, it is a most preferable method for describing TRIP behaviors [5]–[9].However, direct phase-transformation measurement should be carried out under every possible condition. So, a unified constitutive model for TRIP has been provided by authors [10]. This model can describe very well using material parameter of strain hardening rate and strain-rate sensitivity. As aforementioned, however, pre-strain effect is an important factor at the aspect of strength and ductility of 304L stainless steel. Nonetheless, pre-strain dependency is not considered in past models and study. Therefore, previous constitutive model should be modified to reflect pre-strain effect and nonlinear strain hardening rate. In this study, a unified constitutive equation is developed to simulate the material behaviors depending on pre-stain quantities of 304L stainless steel.

A. Elasto-Visco-Plastic constitutive model

The Bodner and Partom elasto-visco-plastic constitutive models are modified to verify the pre-strain effect [11]. According to the BP model, total strain rate $\dot{\varepsilon}^e$ and inelastic strain rate $\dot{\varepsilon}^p$ as follows:

$$\dot{\boldsymbol{\varepsilon}}_{ij} = \dot{\boldsymbol{\varepsilon}}^e_{ij} + \dot{\boldsymbol{\varepsilon}}^p_{ij} \tag{1}$$

$$\dot{\boldsymbol{\varepsilon}}^p_{ij} = D_0 \exp\left\{-\frac{1}{2}\left(\frac{Z}{\sigma_{\text{eff}}}\right)^{2n}\right\}\frac{\sqrt{3}\, s_{ij}}{\sigma_{\text{eff}}} \tag{2}$$

where, D_0 and n are the material parameters, which control the limiting plastic strain rate and rate sensitivity as well as influence the level of stress-strain curves, respectively. Generally, D_0 is the material parameter at 10^4 [11]. Since rate sensitivity n which was calculated at past research using the method suggested by Senchenkov and Tabieva is used for 304L stainless steel of the temperature-dependent rate sensitivity under 110K. And loading history-dependent hardening parameter Z is the internal state variable, indicating the overall resistance level of materials to the plastic flow [12, 13].

$$Z = Z_1 + (Z_0 - Z_1)\exp(mW_p) \tag{3}$$

$$W_p = \int dW_p = \int \sigma_{ij} d\varepsilon^p_{ij} \tag{4}$$

When thermal recovery can be ignored, the parameter Z is expressed as (3). Z_0 and Z_1 are the temperature- and strain rate-dependent material parameters, which indicate the initial value of isotropic hardening and the limiting value of Z, respectively. Parameter m denotes the rate of hardening and W_p denotes the accumulated plastic work defined as (4).

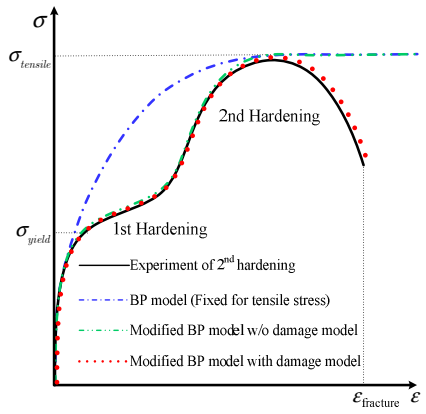

Fig. 4 Stress-strain curves of constitutive models for the expression of 2nd hardening

When the MBP model is adopted as a constitutive model, strain hardening behavior can be expressed effectively by controlling m. Strain hardening rate curve and the method suggested in authors' past research are analyzed and used to identify material parameter m for the expression of pre-strain dependent nonlinear material behavior.

The definition of material parameter m is proposed as a stepwise function that has strain components as variables,

$$m = \left.\frac{m_i - m_{i-1}}{\boldsymbol{\varepsilon}_{i+1} - \boldsymbol{\varepsilon}_i}(\bar{\boldsymbol{\varepsilon}}^p - \boldsymbol{\varepsilon}_{i-1}) + m_{i-1}\right|_{(1\le i\le j)} \tag{5}$$

$$\bar{\boldsymbol{\varepsilon}}^p = \int^t \left|\dot{\boldsymbol{\varepsilon}}^p\right| dt \tag{6}$$

$$m_i = 1 \Big/ \left|\Delta\theta_i\right| \tag{7}$$

where, $\bar{\boldsymbol{\varepsilon}}^p$ stands for accumulated plastic strain. Because the parameter m is expressed as a function of plastic strain on each piecewise step, the hardening function Z as well as m can be controlled in a consistent manner. Namely, once identification of m_i per each jth step is obtained in an overall expression for the whole plastic behavior, m can be easily expressed by (5). m_i is defined as (7) and can be obtained using $\theta - \varepsilon_{ture}$ curve.

At each pre-strain amount, m_i per each jth step is evaluated using the least-squares method according to the $\theta - \varepsilon_{ture}$ curve.

B. Damage model

The damage model based on Bodner's damage model is coupled with elasto-visco-plastic model as shown in (8)

$$\dot{\boldsymbol{\varepsilon}}^p = D_0 \exp\left\{-\frac{1}{2}\left(\frac{Z(1-\omega)}{\sigma_{\text{eff}}}\right)^{2n}\right\}\frac{\sqrt{3}\, s_{ij}}{\sigma_{\text{eff}}} \tag{8}$$

Evolution of material damage variable ω ($0 < \omega < 1$) in this research can be expressed as

$$\dot{\omega} = \frac{b}{h}\left[\ln\left(\frac{1}{\omega}\right)^{(b+1)/b}\right]\omega\,\dot{Q}C_{\text{ZH}} \tag{9}$$

$$\dot{Q} = (\alpha\sigma^+_{\max} + \beta\sigma_{\text{eff}} + \gamma I^+_1)^r \tag{10}$$

b and h of (9) are internal state variables and $\dot{Q}$ is a multi-axial stress function defined as suggested in (10). $\sigma^+_{\max}$, σ_{eff}, and I^+_1 denote the maximum tensile principal stress, effective stress, and the first stress invariant, respectively (positive for tension). α, β, γ, and r are the multi-axial stress control material constants where $\alpha+\beta+\gamma=1$. Hayhurst suggested that $\alpha=0$, $\beta=0.75$, $\gamma=0.25$, and $r=1$ resulted from the uni-axial tensile tests for the general metals [14]. C_{ZH} is Zener and Holloman parameter as defined (11).

$$C_{ZH} = \frac{\dot{\varepsilon}_p}{\dot{\varepsilon}_{ref}} \exp\left(\frac{T_{ref}}{T}\right) \quad (11)$$

where, $\dot{\varepsilon}_{ref}$ and $\dot{\varepsilon}_p$ denote reference strain rate (0.00016/s) and plastic strain rate, respectively. Then T_{ref} and T are set for the reference temperature (room temperature 293K) and environment temperature [10], [15].

C. Modified Elasto-Visco-Plastic Model

MBP model has suggested represent temperature and strain-rate dependency at low temperature. As aforementioned test results, 304L stainless steel has shown sensitive changes at the aspect of strength and ductility depending on the amount of pre-strain and pre-strain temperature. So, it is inevitable to modify the MBP model for the application of pre-strain effect.

In present study, based on MBP model, hardening function (3) is modified considering Z_0 - σ_{yield} and Z_1 - σ_{uts} relation to apply pre-strain temperature and the amount of pre-strain dependency at the aspect of strength and ductility.

As aforementioned, Z_0 and Z_1 are temperature- and strain-rate-dependent material parameters and not pre-strain dependent parameters. Since constant temperature and strain-rate have used during the re-loading tensile test, Z_0 and Z_1 have to be determined as constant values depending on pre-strain temperature. In this regard, authors suggest the pre-strain dependent function α and β which has the relation $\alpha \cdot \sigma_{yield} \propto Z_0$ and $\beta \cdot \sigma_{uts} \propto Z_1$ and can be calculated from Z_0 and Z_1 obtained from numerical analysis. As inputting the pre-strain amount additionally into the initial conditions like temperature and strain-rate, appropriate pre-strain dependent 2nd hardening material behavior can simulate closely. Therefore α and β are applied into hardening function (3). Then (3) is changed to (12) for the expression of pre-strain dependent material behavior.

$$Z = \beta Z_1 + (\alpha Z_0 - \beta Z_1)\exp(mW_p) \quad (12)$$

Analytical study of overall procedure according to modified hardening function is shown below Fig. 5.

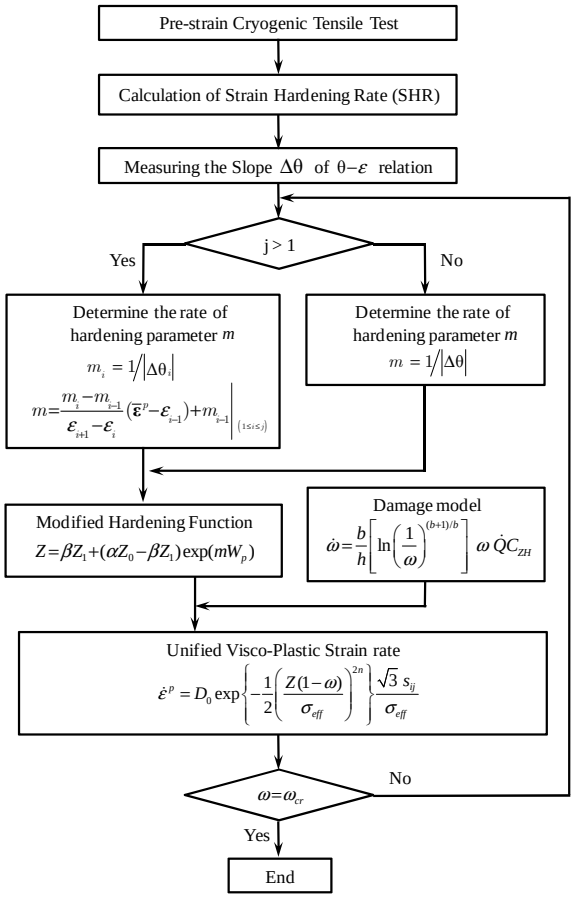

Fig. 5 Overall procedure of present study

V. Numerical Results

The purpose of the developing constitutive model is to establish a numerical algorithm that is applicable for FEA. In this study, in-house FEA code is developed. The in-house FEA code adopt the initial strain method for the incremental formulation [5],

$$\{F^r\} + \{\Delta F\} + \int_V [B]^T [D^e](\{\Delta\varepsilon^{th}\} + \{\Delta\varepsilon^p\})dV = [K^e]\{\Delta u\} \quad (13)$$

Where, $\{F\}^r$ and $\{\Delta F\}$ are the residual force vector and the external force increment vector, respectively. $[B]$ is the strain–displacement matrix, $\{\Delta\varepsilon^{th}\}$ is the initial strain increment vector (the thermal strain increment vector), $\{\Delta\varepsilon^p\}$ is the plastic strain increment vector, $[D^e]$ is the elastic stress-strain relation matrix, $\{\Delta u\}$ is the displacement increment vector, and $[K^e]$ is the elastic stiffness matrix. In order to solve a time-dependent problem considering the effects of temperature and strain rate, the central difference method was used for the time-stepping technique at each increment using (13).

To represent the material damage level precisely, the initial

elasticity tensor E^0_{ijkl}, which is used in $[D^e]$ of (13), should be updated and replaced with the damaged elasticity tensor $E_{ijkl}(\omega)$ at each calculation step. In (14) and (15), ω_{cr} provides the critical value for the determination of the critical state, which corresponds to the absolute loss of load-carrying capacity. A specific value of ω =1.0 would be preferable from a theoretical sense, while practically, ω_{cr} may vary between $\omega_{cr} \cong 0$ for pure brittle fracture to $\omega_{cr} \cong 1$ for pure ductile fracture, but it usually remains of the order of 0.2 to 0.5 and depends sensitively upon the material and the conditions of loading. Therefore, it is suggested to be in the range 0.3 $< \omega_{cr} <$0.5 for the identification of the rupture criterion of each material in this study

$$E_{ijkl}(\omega) = (1-\omega) E^0_{ijkl}, \tag{14}$$

$$E_{ijkl}(\omega) = \begin{Bmatrix} E_{ijkl}(\omega) & \text{for} \quad \omega < \omega_{cr} \\ 0 & \text{for} \quad \omega \geq \omega_{cr} \end{Bmatrix}. \tag{15}$$

VI. Validation and Discussion

The proposed constitutive model has applied to in-house FEA code and verified by comparison test results with FEA results. As shown in Fig. 6, the pre-strain dependent hardening behaviors of 304L stainless steel are simulated very well. Even though each hardening characteristic is different, the numerical results coincide properly for ambient temperatures and low temperatures.

This indicates very meaningful aspects, as follows: (1) the proposed model can describe significant TRIP as well as general hardening, (2) the proposed material parameter identification method can produce reliable numerical results, (3) establishment for the numerical model and parameters are easily done with some simple tensile tests.

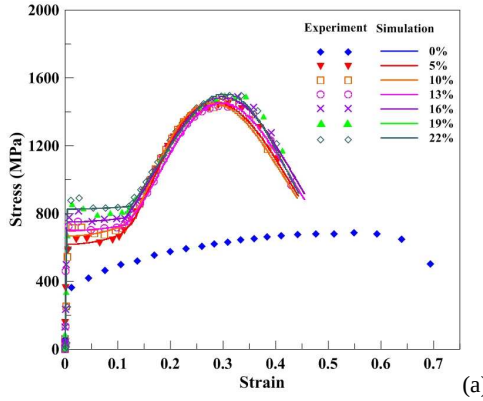

(a)

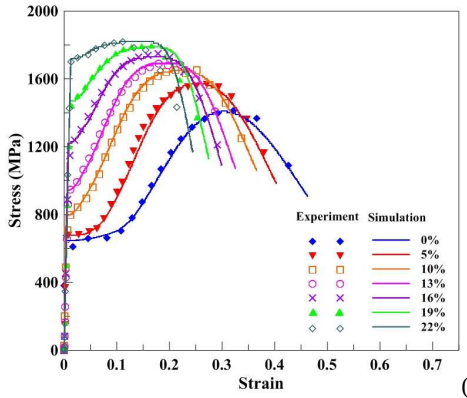

(b)

Fig. 6 Comparison of stress-strain relationship between numerical results and experimental results (a) AL test (b) LL test

VII. Conclusion

In the present study, pre-strain dependent tensile test considering temperature effect was carried out. Moreover, constitutive equations for expressing nonlinear behavior of test results were proposed. Identification methods for material parameters were also suggested. For a representative low temperature application, verification studies were conducted. The main research results can be summarized as follows:

1) In case of pre-strained at ambient temperatures, 304L stainless steel shows increasing tendencies such as yield stress, ultimate tensile stress, and ductility. However, ductility is maintained regardless of the amount of pre-strain.
2) In case of pre-strained at 110K temperatures, 304L shows increasing tendencies similar with the cases of pre-strained under room temperatures in yield stress and tensile stress. But unlike AL test results, the amount of ductility is decreased rapidly.
3) Modified model of Bodner type elasto-visco-plastic model coupled with damage model was suggested. And proposed constitutive equation is validated the simulation results with test results using suggested material parameters.

Acknowledgment

This research was supported by the Basic Science Research Program through the National Research Foundation of Korea (NRF) funded by the Ministry of Education, Science and Technology (2011-0003879). This work was supported by the National Research Foundation of Korea (NRF) grant funded by the Korea government (MEST) (No. 2011-0030667).

References

[1] W.S. Lee, C.F. Lin, "Comparative study of the impact response and microstructure of 304L stainless steel with and without prestrain", *Metall. Mater. Trans. A*, vol. 33, pp. 2801-2810, 2002

[2] Y. Iino, "Effect of small and large amounts of prestrain at 295K on tensile properties at 77K of 304 stainless steel", *JSME Int J., Ser. A*, vol. 35, pp.303-309, 1992

[3] L.T. Robertson, T.B. Hilditch, P.D. Hodgson, "The effect of prestrain and bake hardening on the low cycle fatigue properties of TRIP steel", *Int. J. Fatigue*, vol. 30, pp.587-594, 2008

[4] W. S. Park, S. W. Yoo, M. H. Kim, and J. M. Lee, "Strain-rate effects on the mechanical behavior of the AISI 300 series of austenitic stainless steel under cryogenic environments", *Mater. Des.* Vol. 31, pp. 3630-3640, 2010
[5] K.J. Lee, M.S. Chun, M.H. Kim, J.M. Lee. "A new constitutive model of austenitic stainless steel for cryogenic applications", *Comp Mater Sci.*, vol. 46, pp. 1152-1162, 2009
[6] G.B. Olson, M. Cohen. *Metall. Mater. Trans. A*, vol. 6, pp. 791-795, 1975
[7] Tomita, Y., Iwamoto, T., "Computational prediction of deformation behavior of TRIP steels under cyclic loading", *Int. J. Mech. Sci.*, vol. 43, pp. 2017–2034, 2001
[8] C. Garion, B. Skoczeń, S. Sgobba, "Constitutive modelling and identification of parameters of the plastic strain-induced martensitic transformation in 316L stainless steel at cryogenic temperatures", *Int. J. Plast.*, vol. 22, pp. 1234-1264, 2006
[9] Y. Tomita, T. Iwamoto, *Int. J. Mech. Sci*. vol. 37, no. 12, pp. 1295-1305, 1995
[10] W. S. Park, C. S. Lee, M. S. Chun, M, H. Kim, J. M. Lee, "Comparative study on mechanical behavior of low temperature application materials for ships and offshore structures: Part II – Constitutive model", *Mater Sci Eng A.*, vol. 528, pp. 7560-7569, 2011
[11] Bodner, S. R., *Unified Plasticity for Engineering Applications* .Kluwer Academic/ Plenum Publishers, 2002
[12] L. Durrenberger, J.R. Klepaczko and A. Rusinek, "Constitutive modeling of metals based on the evolution of the strain hardening rate", *J. Eng. Mater. Technol.*, vol. 129, pp.550–558, 2007
[13] I.K. Senchenkov and G.A.Tabieva, "Determination of the parameters of the Bodner-Partom model for thermoviscoplastic deformation of materials", *Int. Appl. Mech.*, vol. 32, pp.132–139, 1996
[14] D.R. Hayhurst and F.A. Leckie, "Constitutive Equation for Creep Damage", *Acta Metall.*, vol. 25, pp.1059-1070, 1977
[15] C. Zener and J.H. Hollomon, *J. appl. Phys*., vol. 15, pp. 22, 1944